Dossier

This paper is a part of the hereunder thematic dossier published in OGST Journal, Vol. 70, No. 1, pp. 3-211 and available online here

Cet article fait partie du dossier thématique ci-dessous publié dans la revue OGST, Vol. 70, n°1, pp. 3-211 et téléchargeable ici

DOSSIER Edited by/Sous la direction de : **B. Leduc et P. Tona**

IFP Energies nouvelles International Conference / Les Rencontres Scientifiques d'IFP Energies nouvelles
E-COSM'12 — IFAC Workshop on Engine and Powertrain Control, Simulation and Modeling
E-COSM'12 — Séminaire de l'IFAC sur le contrôle, la simulation et la modélisation des moteurs et groupes moto-propulseurs

Oil & Gas Science and Technology – Rev. IFP Energies nouvelles, Vol. 70 (2015), No. 1, pp. 3-211

IFP Energies nouvelles

Oil & Gas Science and Technology – Rev. IFP Energies nouvelles, Vol. 70 (2015), No. 1, pp. 55-65

DOI: 10.2516/ogst/2013203

IFP Energies nouvelles International Conference
Rencontres Scientifiques d'IFP Energies nouvelles

E-COSM'12 - IFAC Workshop on Engine and Powertrain Control, Simulation and Modeling
E-COSM'12 - Séminaire de l'IFAC sur le contrôle, la simulation et la modélisation des moteurs et groupes moto-propulseurs

Automotive Catalyst State Diagnosis Using Microwaves

Ralf Moos* and Gerhard Fischerauer

Bayreuth Engine Research Center, Zentrum für Energietechnik, University of Bayreuth, 95447 Bayreuth - Germany
e-mail: functional.materials@uni-bayreuth.de - mrt@uni-bayreuth.de

* Corresponding author

Abstract — *The state of catalysts plays a key role in automotive exhaust gas aftertreatment. The soot or ash loading of Diesel particulate filters, the oxygen loading degree in three-way catalysts, the amount of stored ammonia in SCR catalysts, or the NO_x loading degree in NO_x storage catalysts are important parameters that are today determined indirectly and in a model-based manner with gas sensors installed upstream and/or downstream of the catalysts. This contribution gives an overview on a novel approach to determine the catalyst state directly by a microwave-based technique. The method exploits the fact that the catalyst housing acts as a microwave cavity resonator. As "sensing" elements, one or two simple antennas are mounted inside the catalyst canning. The electrical properties of the catalyst device (ceramic honeycomb plus coating and storage material) can be measured. Preferably, the resonance characteristics,* e.g., *the resonance frequencies, of selected cavity modes are observed. The information on the catalyst interior obtained in such a contactless manner is very well correlated with the catalyst state as will be demonstrated for different exhaust gas aftertreatment systems.*

Résumé — **Diagnostic de l'état de catalyseurs d'automobiles à l'aide de micro-ondes** — L'état des catalyseurs joue un rôle essentiel dans le post-traitement des gaz d'échappement automobiles. Le chargement en suie ou en cendres des filtres Diesel à particules, la teneur en oxygène dans les catalyseurs trois voies, la quantité d'ammoniac stockée dans les catalyseurs SCR ou le niveau de chargement en NO_x dans les catalyseurs de stockage de NO_x sont des paramètres importants déterminés aujourd'hui de manière indirecte et sur la base de modèles avec des capteurs de gaz se trouvant en amont et/ou en aval des catalyseurs. Cette contribution présente une nouvelle approche permettant de déterminer l'état du catalyseur, directement en utilisant une technique à micro-ondes. La méthode exploite le fait que le boîtier du catalyseur agit comme cavité résonnante de micro-ondes. En tant qu'éléments de détection, une ou deux antennes simples sont installées à l'intérieur du conditionnement du catalyseur. Les propriétés électriques du dispositif catalytique (nid d'abeille en céramique plus revêtement et matériau de stockage) peuvent être mesurées. De préférence, les caractéristiques de résonnance, par exemple les fréquences de résonnance, des modes de cavité sélectionnés, sont observées. Les données obtenues de cette manière sans contact, sont très bien corrélées avec l'état du catalyseur, tel que cela sera démontré pour différents systèmes de post-traitement des gaz d'échappement.

INTRODUCTION

Technical Background

Steadily increasing costs for fuel and the pressure on automotive manufacturers from costumers and legislation to reduce CO_2 emissions lead to booming market shares for Diesel passenger cars. Since Diesel engines are operated leanly and Nitrogen Oxides (NO_x) cannot be removed with conventional Three-Way Catalysts, or TWC (Alkemade and Schumann, 2006; Shelef and McCabe, 2000), novel exhaust gas aftertreatment concepts have emerged.

The ammonia selective catalytic reduction process (NH_3-SCR) has been transferred from power plant applications to automotive requirements. For both heavy duty vehicles and passenger cars, systems have already been serialized in the past few years (Koebel *et al.*, 2004; Johnson, 2012). In NH_3-SCR systems, a urea water solution is injected into the exhaust. Ammonia is formed by hydrolysis and serves as a selective reduction agent for NO_x. According to the reaction mechanism, NH_3 is initially adsorbed (stored) in the SCR catalyst. The NO_x reduction (conversion rate) depends strongly on the amount of stored NH_3, especially at low temperatures (Busca *et al.*, 1998; Kröcher *et al.*, 2006; Johnson, 2012).

In NO_x Storage Catalysts (NSC), also known as Lean NO_x Traps (LNT), NO_x is adsorbed and stored in the form of nitrates during a lean phase. Nitrate reduction occurs in a subsequent short rich phase, right before the storage capacity of the NSC is exhausted and NO_x slip occurs (Takeuchi and Matsumoto, 2004).

For both NO_x abatement technologies, NH_3-SCR and NSC, novel exhaust gas sensors that provide information on the state of the catalyst (amount of stored NO_x or NH_3) to supplement the well-known and mature lambda probe would be beneficial for catalyst control.

In order to remove the emitted particulate mass and number, Diesel Particulate Filters (DPF) have been serialized. To avoid clogging, they have to be regenerated regularly to burn off sorbed soot (Twigg and Phillips, 2009). Since regenerations consume fuel, the number of regenerations has to be kept to the minimum. Hence, detailed knowledge of the actual soot loading would be beneficial.

The exhausts of most gasoline-fuelled internal combustion engines are treated by TWC. Only under stoichiometric conditions, *i.e.* with an air-fuel equivalence ratio (also denoted as normalized air-to-fuel ratio, λ) of $\lambda = 1$, all limited exhaust components, like NO_x, hydrocarbons, or carbon monoxide, are converted best. Lambda probes, which are installed upstream and downstream of each catalyst, determine the actual values of λ in the gas phase (Riegel *et al.*, 2002; Twigg, 2007). To buffer rich-to-lean fluctuations, the washcoats of the TWC (honeycomb-like substrate with catalytically active coating) contain large quantities of doped ceria-zirconia solutions as a component for oxygen storage, making use of cerium's two different oxidation states at exhaust temperatures. The Oxygen Storage Capacity (OSC) of a TWC is directly related to the amount of available ceria (Möller *et al.*, 2009). By λ measurements up- and downstream of a TWC, the oxidation degree is calculated by OSC models. Such an indirect characterization of the TWC oxygen loading degree is today's best available technology.

Exhaust Gas Sensors

Many efforts were being made in the past years to develop novel automotive exhaust gas sensors that are sensitive, selective, long-term stable, and cost effective (Riegel *et al.*, 2002; Moos, 2005; Alkemade and Schumann, 2006; Zhuiykov and Miura, 2007; Fergus, 2007; Moos and Schönauer, 2008). However, per today, only sensors based on yttria stabilized zirconia like the binary lambda probe, the wide-band lambda probe (also Universal Exhaust Gas Oxygen sensor, UEGO sensor, or linear lambda probe), and the amperometric NO_x sensor have been serialized. In addition to direct engine control, it is the purpose of these selective exhaust gas sensors to detect the state of the catalyst indirectly, supported by models. "State" in this respect may mean, for instance, the oxygen loading of three-way catalysts, the NO_x loading of NO_x storage catalysts, the NH_3 loading of ammonia-SCR catalysts, the soot loading of Diesel particulate filters, the conversion efficiency, or the sulfur poisoning.

Direct Catalyst State Observation

In the past few years, it was appreciated more deeply that the catalyst state can be determined directly by monitoring the electrical properties of the catalyst coatings themselves. One may classify all works on this topic in two categories:

- a direct but not contactless approach, and
- a direct and contactless, microwave-based approach.

In the first approach, sections of the catalyst coating are typically investigated by impedance spectroscopy. This has been successfully demonstrated to determine *in situ* the oxygen loading degree in TWC formulations based on ceria-zirconia (Reiß *et al.*, 2009, 2011a), to detect *in situ* the NO_x loading state, the regeneration state, the degree of sulfurization, and the thermal aging state of a NO_x storage catalyst based on earth-alkaline

oxides (Moos *et al.*, 2008a), or to determine the ammonia loading in Fe-SCR zeolites with electrical ac measurements (Kubinski and Visser, 2008; Rodríguez-González and Simon, 2010). The soot loading of DPF can be measured as well, even with a local resolution (Hagen *et al.*, 2011). However, the above-described devices are still additional sensors that need to be mounted into the exhaust pipe.

Even more sophisticated and promising is the recent microwave-based approach. It offers the chance to determine the catalyst state directly without the workaround *via* the concentration of a single compound in the exhaust. The microwave-based automotive catalyst state diagnosis technique is based on the dependence of the electrical properties of the catalyst materials on their loading states (Moos, 2010). To a course approximation, the catalyst housing may be considered a PEC (Perfect Electric Conductor) wall enclosing a cavity. Owing to the typical geometrical dimensions, the lowest-order modes in the cavity resonate at low GHz frequencies. The cavity resonator may be coupled to a source and load *via* simple "antennas" such as short stubs or loops which are mounted inside the catalyst canning. Thus, the electrical properties of the catalyst device (ceramic honeycomb plus coating and storage material) can be measured from the outside. Therefore, the measurement method belongs to the large class of Non-Destructive Evaluation (NDE) methods which allow the investigation of the interior of solid bodies by waves propagating in the solid. Here, preferably, the resonance characteristics, *e.g.*, the resonance frequencies, of selected cavity modes are observed. The information on the catalyst interior obtained in such a contactless manner correlates very well with the catalyst state as will be shown for the detection of the oxygen loading of a TWC, the NO_x loading of an NSC, the soot loading of a DPF, and the amount of stored ammonia in an SCR catalyst.

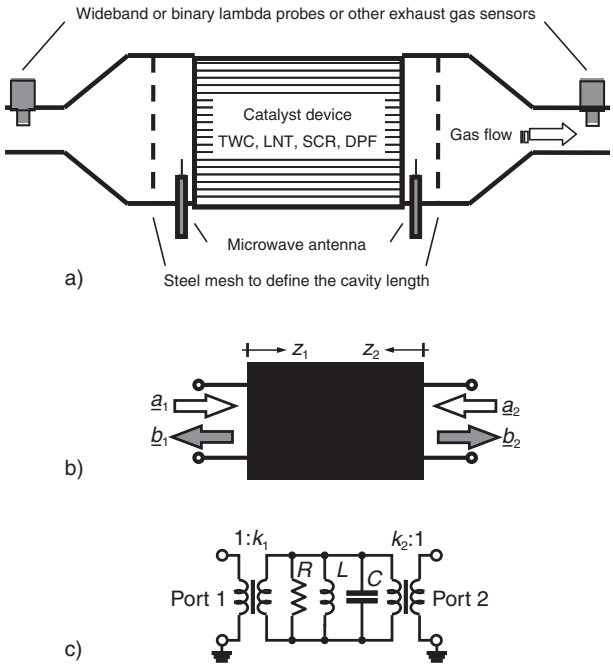

Figure 1

Setup of the microwave-based automotive catalyst state diagnosis. a) Schematic diagram. For research purposes, steel meshes may be inserted as indicated to exactly define the cavity length. The wideband lambda-probes or other exhaust gas sensors are for research purposes only. b) Representation as a microwave two-port with incident and scattered wave amplitudes. c) Equivalent circuit for a narrow frequency band near the resonance frequency of a single cavity mode.

1 MICROWAVE-BASED CATALYST MONITORING

1.1 Principle

As already described, the electrically conducting canning of a catalyst converter (or of a DPF) defines a cavity resonator. Typically, it is coupled to its environment *via* one or two coaxial waveguide feeds (antennas) which are mounted inside the canning (*Fig. 1a*). At microwave frequencies, voltages, currents, and impedances can be neither defined unambiguously nor measured directly. What can be measured are the amplitudes and phase angles of the electric and magnetic field components associated with the electromagnetic waves propagating along a waveguide. For a propagating sinusoidal mode in a uniform waveguide such as a coaxial line, the ratio of the amplitudes of any two field components and the phase difference between any two field components are constant along the waveguide. Hence, the mode can be described unambiguously by a complex-valued scalar wave amplitude:

$$\underline{a} = |\underline{a}| \cdot \mathrm{e}^{-jkz} \tag{1}$$

where k is the wave number and z denotes the coordinate along the waveguide axis ($z = 0$ corresponds to the location of a reference plane which may be chosen freely). It is a common practice to normalize the magnitude of $\underline{a}$ such that it is linked to the time-averaged power transported by the mode by:

$$P = \frac{1}{2}|\underline{a}|^2 \tag{2}$$

The cavity shown in Figure 1a has two interfaces, or ports, that separate it from the environment. A coaxial

cable connected to port i supports an incident wave $\underline{a}_i$ and a scattered wave $\underline{b}_i$ (it is assumed that the cable supports only its fundamental transverse electromagnetic mode in the frequency range of interest, which is certainly true in the lower GHz range; *Fig. 1b*).

As any linear two-port, the housed catalyst is uniquely described by a linear system of equations between the incident and scattered wave amplitudes:

$$\begin{pmatrix} \underline{b}_1 \\ \underline{b}_2 \end{pmatrix} = \begin{pmatrix} \underline{S}_{11} & \underline{S}_{12} \\ \underline{S}_{21} & \underline{S}_{22} \end{pmatrix} \begin{pmatrix} \underline{a}_1 \\ \underline{a}_2 \end{pmatrix} \tag{3}$$

The scattering parameters $\underline{S}_{ij}$ can be easily measured in the laboratory by commercial Vector Network Analyzers (VNA). As a consequence of the normalization (2), the magnitudes squared of the S-parameters are ratios of time-averaged powers. For instance, the magnitude squared of the input reflection coefficient $\underline{S}_{11}$ is the ratio of the average power impressed on port 1 to the average power scattered back at the same port when port 2 is matched ($\underline{a}_2 = 0$). Similarly, the forward and backward transmission coefficients $\underline{S}_{12}$ and $\underline{S}_{21}$ describe the transmission of power from one port to the other through the interior of the cavity resonator.

Figure 1c shows an equivalent circuit which describes the terminal characteristics of the microwave cavity resonator in a narrow frequency band around the resonance frequency of a single cavity mode. (A broadband equivalent circuit consists of many analogous RLC circuits.) There is an unambiguous relationship between the generalized voltages and currents of such an equivalent circuit and the complex wave amplitudes at the interfacing terminals. When the material parameters of the housed catalyst change as a result of electrochemical reactions, this shows up in a change of the equivalent-circuit element values R, L, C, k_1, and k_2 or, equivalently, in a change of the S-parameters $\underline{S}_{ij}$.

Further details of the measurement technique can be found in the literature (Fischerauer *et al.*, 2008, 2010a). Microwave concepts such as electromagnetic waveguides, cavity resonators, and S-parameters are treated in many standard texts (Harrington, 1961). There exists a vast literature on the use of cavity resonators for the measurement of material properties of small samples. This deviates from the present application as the catalyst-filled cavities contain large samples. Still, many basic features of the method can be understood from the standard theory of cavities perturbed by small samples (Sucher and Fox, 1963; Klein *et al.*, 1993; Carter, 2001).

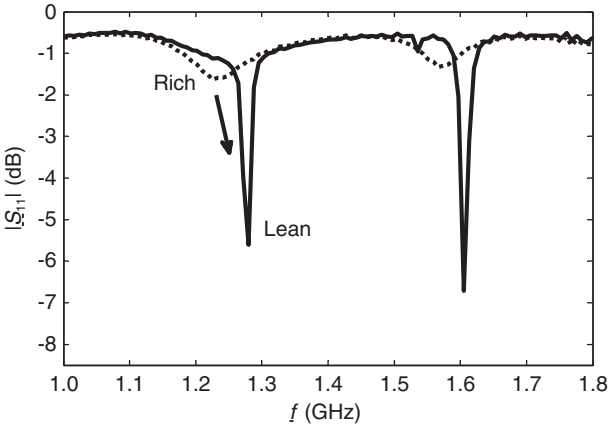

Figure 2

Return loss $|\underline{S}_{11}|$ of a canned TWC in the frequency range in which the two lowest-order cavity modes resonate and at approximately 450°C. Reiß *et al.* (2011b).

1.2 Application to Three-Way Catalysts

As mentioned above, today's gasoline-operated automobiles are equipped with TWC for best conversion of the limited components hydrocarbons, CO, and NO_x. They have to be operated stoichiometrically (at $\lambda = 1$). To buffer air-to-fuel fluctuations, ceria-zirconia solutions are added as oxygen storing materials. Using the signals of lambda probes upstream and downstream of the TWC, the oxidation states of the catalysts are modeled.

Since the electronic conductivity of ceria-zirconia solutions depends on the equilibrium oxygen partial pressure (Boaro *et al.*, 2002), pO_2, which is a measure of the oxygen loading degree (Möller *et al.*, 2009), a direct catalyst state control determining the overall oxygen loading may be possible (Moos *et al.*, 2008b).

A typical resonance spectrum of a TWC operated at steady state conditions in lean and rich exhausts is shown in Figure 2 (Reiß *et al.*, 2011b). Both the resonance frequency and the magnitude of the reflection coefficient $\underline{S}_{11}$ at the resonance frequency may be an appropriate signal feature from which the oxygen loading of the TWC can be inferred.

Using either the shift of the resonance frequency f_{res} of a suitable cavity mode or the attenuation at this frequency, one may determine the amount of loaded oxygen. This has been shown by careful titrations in the engine dynamometer as well as in the lab test bench (Reiß *et al.*, 2011a, b). The system is not sensitive to other exhaust components such as H_2, CO_2, or CO (Reiß *et al.*, 2011c). However, as both the size of the cavity and

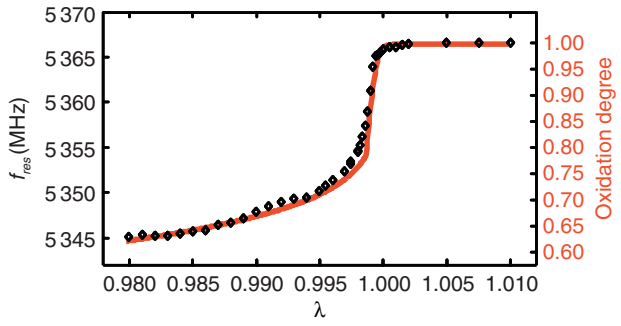

Figure 3

Resonance frequency (symbols) and oxidation degree after the model from Möller *et al.* (2009) (solid line, red) as functions of the λ of the feed gas. $T = 450$°C. For further details see Beulertz *et al.* (2013). From Beulertz *et al.* (2013), with kind permission from Springer Science + Business Media.

the electrical conductivity of the catalyst materials depend on temperature, temperature effects occur and may need to be compensated (Reiß, 2012).

Very recently is has been shown in laboratory experiments that one can realize a low-emission engine control without lambda probes solely by using the resonance frequency of one cavity mode of the housed TWC operated as microwave one-port, *i.e.*, coupled by a single antenna, which means that one can only measure one *S*-parameter, viz., $\underline{S}_{11}$ (Beulertz *et al.*, 2012). In this scheme, the resonance frequency serves as the controlled variable of the closed-loop control system, but, of course, it is a direct measure of the oxygen loading degree of the catalyst.

Figure 3 shows how the oxidation degree of ceria, the resonance frequency, and λ in equilibrium depend on each other. It is noteworthy to mention that, with this method, the model of Möller *et al.* (2009), which predicted the oxidation state of ceria in TWC in much more detail than earlier models, could have been validated for the first time directly, without titration.

1.3 Application to NO_X Storage Catalysts

Nitrogen oxide removal (NO_x = NO and NO_2) from exhausts of leanly operated engines is not possible by TWC, since the reducing components CO, H_2, and hydrocarbons are oxidized by O_2 instead of being used for NO_x reduction (Alkemade and Schumann, 2006). To overcome this, the NSC has been originally developed for direct injection gasoline engines that are operated in the lean mode (Takeuchi and Matsumoto, 2004) and has later been applied also for Diesel exhaust gas aftertreatment (Kašpar *et al.*, 2003). During a lean phase, NO_x is oxidized, sorbed, and stored in the form of nitrates (some minutes). Just before the NO_x storage capacity is exhausted and the catalyst begins to let NO_x pass, the engine is switched to the rich operation mode (some seconds) and the formed nitrates are reduced to N_2 (Epling *et al.*, 2004). Usually, NSC-based exhaust gas aftertreatment catalysts cannot be operated in an open loop. A NO_x sensor is mounted downstream of the NSC to detect NO_x breakthroughs, acts as part of a closed-loop control system and thus helps to prevent overloading of the NSC. A lambda probe ensures that the regeneration period is only as long as necessary to avoid CO or hydrocarbon breakthroughs.

The microwave-based approach may detect the NO_x loading degree directly. Initial tests were conducted in a lab test bench (Moos *et al.*, 2009). Microwave spectra were taken from 1 to 4 GHz for fully loaded and depleted NSC. Compared to the TWC, in this case, a less pronounced shift in the resonance frequencies and a slight broadening of the resonance peaks were observed. The relative resonance frequency changes due to NO_x loading, $\Delta f_{res}/f_{res}$, were compared for all resonances and the one with the highest effect of NO_x was used for further studies. The transient behavior of the resonance peak at ca. 2.615 GHz is shown in Figure 4 by way of an example. The following section is a summary of an extensive study (Fremerey *et al.*, 2011).

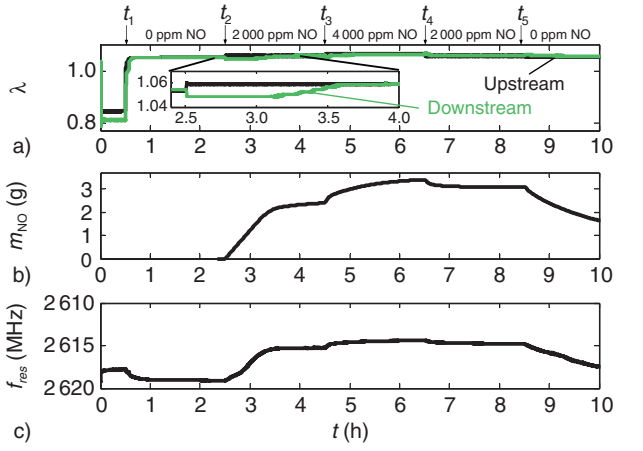

Figure 4

NO_x loading of an NSC monitored by the microwave-based technique at 300°C. Time responses of a) the normalized air-to-fuel ratios λ up- and downstream of the catalyst, b) the NO_x loading, and c) the resonance frequency f_{res} of the mode resonating at about 2.615 GHz. Fremerey *et al.* (2011).

At the beginning of the test run, a NO_x-free lean base gas was applied to the NSC (5% CO_2, 1% O_2, and 8% H_2O in N_2) at $t = t_1$ after a previous rich regeneration phase (1% H_2, 100 ppm C_3H_8, 5 000 ppm CO and 8% H_2O in N_2) to fully remove stored NO_x. Starting at $t = t_2$, 2 000 ppm of NO was added to the base gas for 2 h. The concentration of NO in the feed gas was increased to 4 000 ppm at $t = t_3$. At $t = t_4$, the NO concentration was switched back to 2 000 ppm, and after $t = t_5$, the feed gas consisted of only base gas without NO.

It is evident from Figure 4a, that the wideband lambda sensor upstream of the catalyst quickly reacts to the switch from rich to lean feed gas composition at $t = t_1$, whereas the sensor downstream has a slightly delayed response. Its signal remains around $\lambda \approx 1$ for several minutes before it reaches the same value as the sensor upstream of the catalyst. This delay is caused by the oxygen storage component in the NSC. As soon as the NSC is completely loaded with oxygen, both wideband lambda sensor signals coincide. After the addition of NO at $t = t_2$, the λ of the feed gas increases a little as indicated by the upstream lambda probe (highlighted in the inset). At the same time, the λ downstream of the NSC drops a bit. This is not surprising since oxygen is required for the storage reaction and, therefore, as long as the NSC stores NO_x, the downstream λ should be lower than without NO in the feed. At $t \approx 3.5$ h, the catalyst is saturated (for 2 000 ppm NO in the feed), and no NO_x can be stored anymore. A similar behavior occurs after $t = t_3$, when the NO concentration is further increased. Owing to the chemical equilibrium of the storage reaction, the storage capacity of the NSC is greater at higher NO concentrations and more NO_x can be stored. Analogously, the equilibrium changes back to lower loading states when NO is decreased to 2 000 ppm again at $t = t_4$ as well as to 0 ppm at $t = t_5$. In both cases NO_x, desorbs from the NSC.

By balancing the nitrogen oxide concentrations upstream and downstream of the NSC during the loading period, one should be able to obtain information on the amount of NO_x stored in the NSC (*Fig. 4b*). The same picture is given by the resonance frequency, f_{res}, in Figure 4c. One can clearly see the difference of the signal between the rich and lean gas atmospheres soon after $t = t_1$, which is caused by the oxygen storage capability of the NSC formulation. As known from TWC (see above), the oxidation state of the oxygen storage component has a major influence on the microwave absorption. At the beginning of the NO_x storage at $t = t_2$, f_{res} decreases continuously until $t \approx 3.3$ h. From then on, it remains constant. The curve strongly resembles the NO mass loading curve in Figure 4b. A further increased NO concentration in the feed gas ($t_3 < t < t_4$) also affects the microwave signal, indicating an increasing mass of stored NO in the NSC.

In summary, these results give a first hint that the NO_x loading of the NSC can be measured directly by the contactless microwave-based monitoring technique. However, the effect is by far smaller than for TWC. Cross effects of the oxygen loading may be high enough to thwart the entire approach.

1.4 Application to NH_3-SCR Catalysts

In SCR systems, an aqueous urea solution is injected into the exhaust. It decomposes to NH_3 which then serves as a reducing agent. In the SCR-catalyst, NO_x is selectively reduced by NH_3 to N_2 and H_2O. All major SCR mechanisms are based on an initial NH_3 storage step before NH_3 reacts with NO or NO_2 (Nova *et al.*, 2006; Busca *et al.*, 1998). The NO_x conversion depends on temperature and on the amount of NH_3 stored in the SCR catalyst (Busca *et al.*, 1998; Ciardelli *et al.*, 2007). To avoid NH_3 breakthroughs, today's control systems use a model-based estimation of the NH_3 loading (Schuler *et al.*, 2009).

Since zeolite materials change their electrical impedance when NH_3 is stored (Kubinski and Visser, 2008), it can be expected that the microwave response of zeolite-based SCR catalysts depends on their NH_3 loading degree. This was investigated in literature (Reiß *et al.*, 2011d) and will be summarized in the following section.

A similar test as described above for NSC was conducted with a zeolite containing iron. In a key experiment (*Fig. 5*), a fully NH_3-free catalyst was loaded with NH_3. Then, NO was added and the feed ratio $\alpha = c_{NH_3}/c_{NO}$ was reduced stepwise. Between $t = t_1$ and $t = t_2$, only NH_3 was added to the base gas. It loaded the SCR catalyst. At $t = t_a$, the catalyst became fully NH_3-loaded as indicated by an NH_3 breakthrough. The outlet NH_3 concentration decreased with increasing NO concentration until the catalyst was NH_3-free at $t = t_b$. The mass of stored ammonia, m_{NH_3}, was balanced (*Fig. 5c*). The plot of the resonance frequency of a mode resonating at about 2.92 GHz demonstrates the good correlation between m_{NH_3} and f_{res} (*Fig. 5d*).

The influence of sorbed water was investigated as well. It was found that some resonance modes depend strongly on the water concentration, whereas others are mainly affected by the NH_3 loading. One has to keep in mind that the various resonance modes are standing waves which differ from each other by the locations of the nodes and maxima of the instantaneous field

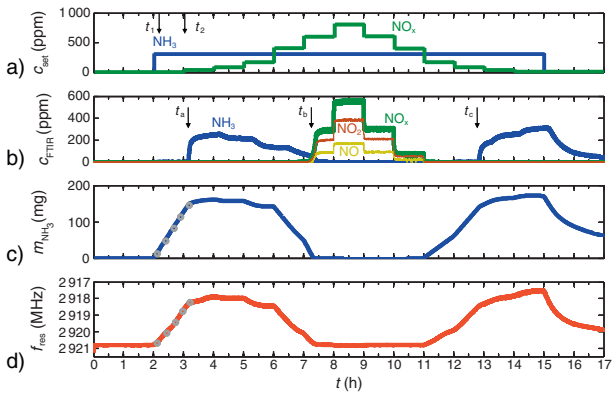

Figure 5

Determination of the NH_3 loading degree with a microwave-based setup. Conditions: T = 300°C, base gas 10% O_2 and 7% H_2O in N_2. NH_3 and NO added as indicated. a) NH_3 and NO dosing; b) outlet FTIR analysis; c) stored NH_3 mass, m_{NH_3}; d) resonance frequency of the mode resonating at about 2.92 GHz. From Reiß *et al.* (2011d), with kind permission from of Wiley-VCH Verlag GmbH & Co. KGaA, Weinheim.

patterns. If the catalyst conductivity increases in a region where a mode has an electric field node, this mode will not respond to the conductivity change. In contrast, a mode with an electric field maximum in the region considered will respond strongly. The resonance modes that depend selectively on the NH_3 loading are suited best for future engine tests. In summary, one can determine the NH_3 loading of an SCR catalyst, but one has to keep in mind that relative resonance frequency shifts between the fully loaded and the unloaded state are smaller by a factor of ten in comparison to TWC.

1.5 Application to DPF Soot Loading Determination

Currently, a model based on the pressure drop over the DPF is utilized to estimate the soot loading (Rose and Boger, 2009). However, a more precise tool would be helpful. While the microwave-based catalyst state diagnosis is in an initial research state, the same principle has been applied for soot loading determination of Diesel particulate filters and is now in a serial development stage. Besides institutional research (Fischerauer *et al.*, 2010b; Feulner *et al.*, 2012), at least two suppliers (Sappok *et al.*, 2010; *General Electric*, 2011) and some automotive manufacturers published recent work or applied for patents (Knitt and DeCou, 2007; Walton, 2007; Gonze *et al.*, 2010; Hansson and Ingeström, 2012; Kulkarni *et al.*, 2012) on the microwave-based soot load detection. The following section summarizes the findings and the differences to the catalyst state diagnosis.

Since soot loading in DPF increases the filter conductivity by orders of magnitude (Hagen *et al.*, 2010), one observes effects as great as in TWC. In order to suppress the possible influence of soot deposition at the coupling antenna, one may use a single waveguide feed located downstream of the DPF where the exhaust is almost soot-free. The spectra of the reflection parameter look very similar to those encountered in the TWC case (*Fig. 6*). The higher the soot load, the more the resonance frequency is shifted towards lower values and the more the resonance peaks broaden, *i.e.* the Full Width at Half Maximum (FWHM) increases (Fischerauer *et al.*, 2010b). In other words, the quality factors, or Q, of the resonance modes decrease, which is always a consequence of higher losses. It has been clearly demonstrated that uncoated and filters coated with an oxidizing material behave equally (Fischerauer *et al.*, 2010b).

The results in Fischerauer *et al.* (2010b) were obtained only at room temperature but they could be reproduced for several different DPF devices. Very recently, dynamic tests were conducted in a dynamometer test bench. By tracing one resonance peak, it should be possible to estimate the soot mass continuously from the magnitude of the reflection coefficient $\underline{S}_{11}$ at a resonance, the resonance frequency, or the resonance Q. In the following, special attention will be paid to the frequency shift, as this parameter appears to be the most promising one for an application in the engine exhaust.

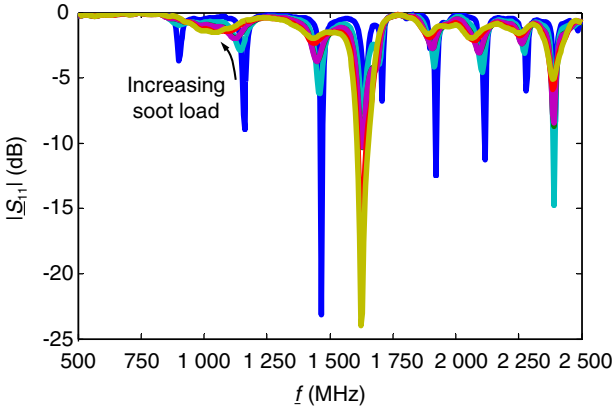

Figure 6

Return loss $|\underline{S}_{11}|$ at different levels of soot-loading in the frequency range from 0.5 to 2.5 GHz. Adapted from Feulner *et al.* (2012).

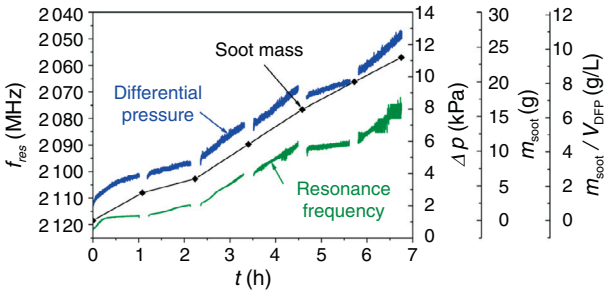

Figure 7

Resonance frequency of a selected cavity mode (f_{res}), differential pressure (Δp), and relative soot mass during constant operation conditions (2 350 rpm, 20% load, $T \approx 220°C$). Pauses indicate time intervals in which the filter was weighed. From Feulner *et al.* (2013a), with kind permission from Springer Science + Business Media.

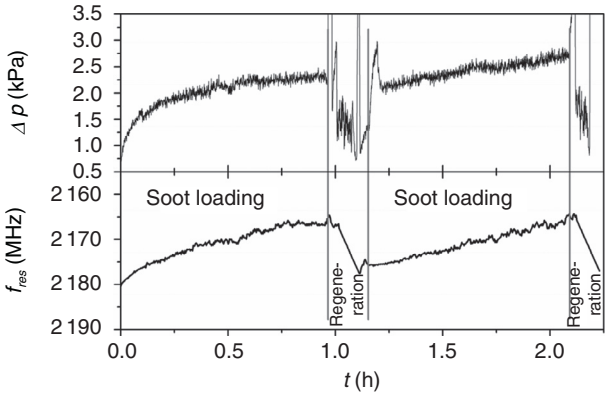

Figure 8

Differential pressure (upper graph) and resonance frequency of a selected cavity mode (lower graph) during two cycles of loading at constant speed and load (T ≈ 350°C) and during regeneration (idle phase with external burner). From Feulner *et al.* (2013a), with kind permission from Springer Science + Business Media.

In a typical experiment, the DPF was continuously soot-loaded in a test bench at constant speed and load (*Fig. 7*). During pauses every hour, the DPF was dismounted, weighed, and mounted again in order to determine the actual soot mass inside the filter. As can be seen, a very good agreement between differential pressure (Δp), resonance frequency, and relative soot mass (in g/L) can be observed.

In another test, soot mass increase during loading and regeneration was observed. Here, regeneration was carried out at engine idle by increasing the exhaust gas temperature with a Diesel-fueled burner upstream of the DPF. The results in Figure 8 confirm the good correlation of differential pressure (upper curve) and resonance frequency (lower curve) not only during soot accumulation in the DPF, but also during filter regeneration. After each regeneration (in *Fig. 8* at 1.1 h and at 2.2 h), both measuring methods indicate a soot-free DPF.

Hansson and Ingeström (2012), report on the *General Electric* system that uses two antennas and considers the attenuation losses. It has been shown that an average value of $|\underline{S}_{21}|$ over a distinct frequency range is also a good indicator for the soot loading. Cross-effects of temperature and mass flow are also studied. Similar to the TWC, the temperature dependence cannot be neglected and needs to be corrected. The space velocity seems to affect the average $|\underline{S}_{21}|$ value only marginally. These results have been independently confirmed by Feulner *et al.* (2013b) on a separate system.

The feasibility of the microwave-based approach for DPF soot loading has been demonstrated by several groups. Future work needs to address interfering effects like the influence of humidity, which modifies the soot, or the dependence on the exhaust temperature. It has also been investigated whether soot and ash loading can be distinguished. It would be beneficial if substrates of electrically conducting silicon carbide could be monitored as well.

1.6 Comparison of the Magnitude of the Resonance Frequency Change for Different Systems

To compare the influences of the loading states on the resonance frequency changes for different exhaust gas aftertreatment systems, one may define a relative measure (or figure of merit) by:

$$F = \frac{|\Delta f_{res}|}{f_{res}} \cdot \frac{10^6 \text{ ppm}}{100\%} \tag{4}$$

here, Δf_{res} is the resonance frequency difference between the fully loaded state (100% loaded, "full") and the unloaded state (0%, "empty"). f_{res} denotes the resonance frequency in the fully loaded state. Therefore the relative measure F, which may also be considered as a relative sensitivity, expresses the resonance frequency shift in ppm per % (relative) load of NO_x, NH_3, O_2, or soot in the respective catalyst or filter devices. The most prominent effect occurs in DPF. Feulner *et al.* (2013b) has shown very recently that the frequency of the first resonance mode changes at an exhaust temperature of 235°C from 1 235 to 1 178 MHz when the aluminum titanate DPF gets loaded with 4.5 g/L soot (uncoated DPF, ∅5.66" × 6"). If one assumes a maximum acceptable soot load of 10 g/L one would obtain F = 1 025 ppm/% soot load. If only 5 g/L can be tolerated, the resonance frequency still changes by about 500 ppm/%

(or 600 kHz/%) soot load. At the moment, interfering parameters like adsorbed water are under study. In TWC, a marked resonance frequency change can be found as well. For a platinum-coated, ceria-zirconia-containing TWC (diameter 4.66" × 5") at 450°C, F can reach values of almost 300 ppm/% oxygen load (Reiß *et al.*, 2011c). Since the resonance frequency change strongly depends on the effective conductivity change of the catalyst or filter material, it becomes clear that a system like a DPF, in which the conductivity changes by orders of magnitude from almost zero to a very high value because of soot loading, shows a much more pronounced response than a ceria-zirconia coated cordierite substrate (TWC). After all, the conductivity of ceria-zirconia changes only by approximately three orders of magnitude between an oxidized and reduced state (Izu *et al.*, 2008). It has been known for many years that zeolites change their conductivity with ammonia loading (Simon *et al.*, 1998; Rodríguez-González and Simon, 2010), but these effects are in the order of only half a magnitude. Therefore, it is astonishing that for SCR catalysts effects in the range of 50 ppm/% ammonia load occur at 300°C (Reiß *et al.*, 2011d). In recent but yet unpublished work, we even found 80 ppm/% for serial type Cu-Chabazite zeolites at 200°C. However, it is questionable, whether such a sensitivity is high enough to measure the ammonia load accurately, especially if one considers that water adsorption as well as temperature also affect the electrical properties of zeolites. If one calculates the sensitivity for NSC from the data of Fremerey 2011, $F \approx 11$ ppm/% can be found, a value which seems by far too low for real-world applications but which can be explained if one keeps in mind that the conductivity of the NSC coating changes only by a few tens % from the NO_x-depleted to the fully NO_x-loaded state (Moos *et al.*, 2008a).

CONCLUSION

We have given an overview of the state of the art in the microwave-based catalyst state observation technique. Although the application of the method to the *in situ* observation of catalysts and other electrochemical systems is relatively young, it has already attracted much attention. In contrast to the conventional lambda probes, NO_x sensors, or ammonia sensors, the key parameter "catalyst state" can be determined directly. The state of the art as presented in this paper can be summarized as follows: firstly, it has been demonstrated for various systems (TWC, LNT, SCR catalyst, DPF) that the method is applicable in principle. Both test bench and dynamometer test runs have proven that suitable features of the microwave signals (S-parameters) correspond very well with catalyst states obtained indirectly by physical quantities such as lambda values upstream and downstream of a TWC or differential pressure and soot mass in a DPF. Secondly, system-level simulations have indicated that the microwave-based look into the catalysts allows closed-loop control schemes with better characteristics than are possible with the current indirect (model-based) measurement methods. Thirdly, the demonstrator setups rely heavily on laboratory equipment and as such cannot be implemented in actual vehicles. And finally, some influencing effects such as interfering analyte concentrations or temperature have been studied and quantified. However, neither can this be called exhaustive nor is it appropriate to state definitively that one can cope with the influencing effects in a manner satisfactory for practical applications. Further investigations are required.

Therefore, if one intends to bring such a system into serial production, many issues need to be solved: the influence of temperature, the effect of noise factors, the long-term stability of the coupling antenna, and, of course, the cost aspects of the entire system including electronics. As to the latter, it may be remarked that, fortunately, the low GHz range is already used for communications purposes (cellular phones, Wi-Fi, bluetooth, wireless sensor networks, etc.). As a result, the required circuitry has become quite inexpensive. There can be no doubt, therefore, that it is possible to replace the laboratory equipment used so far (in particular, the VNA) by far less expensive customized circuitry. It remains to be seen which increase in measurement uncertainty this step will incur. Also, one has to carefully calculate whether the possible advantages of such a system, like reduced catalyst volume, reduced amount of noble metals, omission of one exhaust gas sensor, and improved accuracy of the catalyst state model, will outweigh the additional cost.

ACKNOWLEDGMENTS

The authors gratefully acknowledge financial support by the German research foundation (DFG) under grants Fi 956/3-2, Fi 956/5-1, MO 1060/6-2, and MO 1060/13-1. They thank *Umicore AG & Co. KG*, for supporting parts of the work (Jürgen Gieshoff, Martin Rösch, Martin Votsmeier, in alphabetical order). Highly acknowledged are contributions from students and research assistants at the Bayreuth Engine Research Center (BERC), especially (in alphabetical order) Gregor Beulertz, Markus Feulner, Gunter Hagen, Sebastian Reiß, and Sebastian Schödel.

REFERENCES

Alkemade U.G., Schumann B. (2006) Engines and exhaust after treatment systems for future automotive applications, *Solid State Ionics* **177**, 2291-2296.

Beulertz G., Votsmeier M., Herbst F., Moos R. (2012) Replacing the lambda probe by radio frequency-based in-operando three-way catalyst oxygen loading detection, *The 14th International Meeting on Chemical Sensors*, Nuremberg, Germany, doi: 10.5162/IMCS2012/P2.2.7.

Beulertz G., Fritsch M., Fischerauer G., Herbst F., Gieshoff J., Votsmeier M., Hagen G., Moos R. (2013) Microwave Cavity Perturbation as a Tool for Laboratory *in Situ* Measurement of the Oxidation State of Three Way Catalysts, *Topics in Catalysis* **56**, 405-409.

Boaro M., Trovarelli A., Hwang J.-H., Mason T.O. (2002) Electrical and oxygen storage/release properties of nanocrystalline ceria–zirconia solid solutions, *Solid State Ionics* **147**, 85-95.

Busca G., Lietti L., Ramis G., Berti F. (1998) Chemical and mechanistic aspects of the selective catalytic reduction of NO_x by ammonia over oxide catalysts: A review, *Applied Catalysis B: Environmental* **18**, 1-36.

Carter R.G. (2001) Accuracy of Microwave Cavity Perturbation Measurements, *IEEE Trans. MTT* **49**, 918-923.

Ciardelli C., Nova I., Tronconi E., Chatterjee D., Bandl-Konrad B., Weibel M., Krutzsch B. (2007) Reactivity of NO/NO_2–NH_3 SCR system for Diesel exhaust aftertreatment: Identification of the reaction network as a function of temperature and NO_2 feed content, *Applied Catalysis B: Environmental* **70**, 80-90.

Epling W.S., Campbell L.E., Yezerets A., Currier N.W., Parks J.E. (2004) Overview of the Fundamental Reactions and Degradation Mechanisms of NOx Storage/Reduction Catalysts, *Catal. Rev.* **6**, 163-245.

Feulner M., Hagen G., Müller A., Brüggemann D., Moos R. (2012) In-Operation Monitoring of the Soot Load of Diesel Particulate Filters with a Microwave Method, *The 14th International Meeting on Chemical Sensors*, Nuremberg, Germany. doi: 10.5162/IMCS2012/P2.2.6.

Feulner M., Hagen G., Piontkowski A., Müller A., Fischerauer G., Brüggemann D., Moos R. (2013a) In-Operation Monitoring of the Soot Load of Diesel Particulate Filters - Initial Tests, *Topics in Catalysis* **56**, 483-488.

Feulner M., Müller A., Hagen G., Brüggemann D., Moos R. (2013b) Microwave-Based Diesel Particulate Filter Monitoring – Soot Load Determination and Influencing Parameters, Sensor 2013, *Proceedings of the 16th International Conference on Sensors and Measurement Science*, Nuremberg, Germany. doi:10.5162/sensor2013/P4.1.

Fergus J.W. (2007) Solid electrolyte based sensors for the measurement of CO and hydrocarbon gases, *Sensors and Actuators B: Chemical* **122**, 683-693.

Fischerauer G., Spörl M., Gollwitzer A., Wedemann M., Moos R. (2008) Catalyst State Observation *via* the Perturbation of a Microwave Cavity Resonator, *Frequenz* **62**, 180-184.

Fischerauer G., Spörl M., Reiß S., Moos R. (2010a) Microwave-Based Investigation of Electrochemical Processes in Catalysts and Related Systems, *Technisches Messen* **77**, 419-427.

Fischerauer G., Förster M., Moos R. (2010b) Sensing the Soot Load in Automotive Diesel Particulate Filters by Microwave Methods, *Measurement Science and Technology* **21**, 035108.

Fremerey P., Reiß S., Geupel A., Fischerauer G., Moos R. (2011) Determination of the NO_x Loading of an Automotive Lean NO_x Trap by Directly Monitoring the Electrical Properties of the Catalyst Material Itself, *Sensors* **11**, 8261-8280.

General Electric (2011) Accusolve Diesel Particulate Filter (DPF) Soot Sensor, Available at: http://www.ge-mcs.com/download/temperature/Accusolve_Soot_Sensor.pdf.

Gonze E.V., Kirby K.W., Phelps A., Gregoire D.J. (2010) Apparatus and Method for Onboard Performance Monitoring of Exhaust Gas Particulate Filter, *US Patent Application US 2010/0180577A1*.

Hagen G., Feistkorn C., Wiegärtner S., Heinrich A., Brüggemann D., Moos R. (2010) Conductometric Soot Sensor for Automotive Exhausts: Initial Studies, *Sensors* **10**, 1589-1598.

Hagen G., Piontkowski A., Müller A., Brüggemann D., Moos R. (2011) Locally resolved *in-situ* detection of the soot loading in Diesel particulate filters, *IEEE SENSORS 2011 Conference*, Limerick, Ireland. doi: 10.1109/ICSENS.2011.6126979.

Hansson J., Ingeström V. (2012) A Method for Estimating Soot Load in a DPF Using an RF-based Sensor, *Master Thesis*, U. of Linköping, Sweden, Available at: http://liu.diva-portal.org/smash/record.jsf?pid=diva2:535349.

Harrington R.F. (1961) *Time-Harmonic Electromagnetic Fields*, McGraw-Hill, New York.

Izu N., Oh-hori N., Shin W., Matsubara I., Murayama N., Itou M. (2008) Response properties of resistive oxygen sensors using $Ce_{1-x}Zr_xO_2$ (x = 0.05, 0.10) thick films in propane combustion gas, *Sensors and Actuators B: Chemical* **130**, 105-109.

Johnson T. (2012) Vehicle Emissions Review – 2012, *Directions in Engine-Efficiency and Emissions Research (DEER) Conference*, Dearborn, Michigan, 16-19 Oct, Available at: https://www1.eere.energy.gov/vehiclesandfuels/pdfs/deer_2012/wednesday/presentations/deer12_johnson.pdf.

Kašpar J., Fornasiero P., Hickey N. (2003) Automotive catalytic converters: Current status and some perspectives, *Catalysis Today* **77**, 419-449.

Klein O., Donovan S., Dressel M., Grüner G., Holczer K. (1993) Microwave Cavity Perturbation Technique: Part I-III, *Int. J. of Infrared and Millimeter Waves* **14**, 12, 2423-2517.

Knitt A.A., DeCou M.T. (2007) Radio frequency particulate sensing system, *US Patent Specification* US 7,253,641.

Koebel M., Elsener M., Kröcher O., Schär C., Röthlisberger R., Jaussi F., Mangold M. (2004) NO_x Reduction in the Exhaust of Mobile Heavy-Duty Diesel Engines by Urea-SCR, *Topics in Catalysis* **43**, 30-31.

Kröcher O., Devadas M., Elsener M., Wokaun A., Söger N., Pfeifer M., Demel Y., Mussmann L. (2006) Investigation of the selective catalytic reduction of NO by NH_3 on Fe-ZSM5 monolith catalysts, *Applied Catalysis B: Environmental* **66**, 208-216.

Kubinski D.J., Visser J.H. (2008) Sensor and method for determining the ammonia loading of a zeolite SCR catalyst, *Sensors and Actuators B: Chemical* **130**, 425-429.

Kulkarni V.P., Leustek M.E., Michels S.K., Nair R.N., Snopko M.A., Knitt A.A. (2012) Ash Detection in Diesel Particulate Filter, *US Patent Application* US 2012/0017570 A1.

Matsumoto S. (2004) Recent advances in automobile exhaust catalysts, *Catalysis Today* **90**, 183-190.

Möller R., Votsmeier M., Onder C., Guzzella L., Gieshoff J. (2009) Is oxygen storage in three-way catalysts an equilibrium controlled process? *Applied Catalysis B: Environmental* **91**, 30-38.

Moos R. (2005) A Brief Overview on Automotive Exhaust Gas Sensors Based on Electroceramics, *International Journal of Applied Ceramic Technology* **2**, 401-413.

Moos R., Schönauer D. (2008) Recent Developments in the Field of Automotive Exhaust Gas Ammonia Sensing, *Sensor Letters* **6**, 821-825.

Moos R., Zimmermann C., Birkhofer T., Knezevic A., Plog C., Busch M.R., Ried T. (2008a) Sensor for Directly Determining the State of a NO_x Storage Catalyst, *SAE paper* 2008-01-0447.

Moos R., Spörl M., Hagen G., Gollwitzer A., Wedemann M., Fischerauer G. (2008b) TWC: Lambda control and OBD without lambda probe - an initial approach, *SAE Paper* 2008-01-0916.

Moos R., Wedemann M., Spörl M., Reiß S., Fischerauer G. (2009) Direct Catalyst Monitoring by Electrical Means: An Overview on Promising Novel Principles, *Topics in Catalysis* **52**, 2035-2040.

Moos R. (2010) Catalysts as Sensors—A Promising Novel Approach in Automotive Exhaust Gas Aftertreatment, *Sensors* **10**, 6773-6787.

Nova I., Ciardelli C., Tronconi E., Chatterjee D., Bandl-Konrad B. (2006) NH_3–NO/NO_2 chemistry over V-based catalysts and its role in the mechanism of the Fast SCR reaction, *Catalysis Today* **114**, 3-12.

Reiß S., Wedemann M., Moos R., Rösch M. (2009) Electrical *in situ* characterization of three-way catalyst coatings, *Topics in Catalysis* **52**, 1898-1902.

Reiß S., Spörl M., Hagen G., Fischerauer G., Moos R. (2011a) Combination of wirebound and microwave measurements for *in-situ* characterization of automotive three-way catalysts, *IEEE Sensors Journal* **11**, 434-438.

Reiß S., Fischerauer G., Moos R. (2011b) Radio frequency-based determination of the oxygen loading of automotive three-way catalysts, *Sensor 2011*, Nuremberg, Germany. doi: 10.5162/sensor11/d4.1.

Reiß S., Wedemann M., Spörl M., Fischerauer G., Moos R. (2011c) Effects of H_2O, CO_2, CO., and flow rates on the RF-based monitoring of three-way catalysts, *Sensor Letters* **9**, 316-320.

Reiß S., Schönauer D., Hagen G., Fischerauer G., Moos R. (2011d) Monitoring the ammonia loading of zeolite-based ammonia SCR catalysts by a microwave method, *Chemical Engineering and Technology* **34**, 791-796.

Reiß S. (2012) Direkte Zustandssensorik von Automobilabgaskatalysatoren, R. Moos G. Fischerauer (Hrsg.), *Bayreuther Beiträge zur Sensorik und Messtechnik*, **9**, Shaker-Verlag, Aachen. Thesis, Universität Bayreuth.

Riegel J., Neumann H., Wiedenmann H.-M. (2002) Exhaust Gas Sensors for Automotive Emission Control, *Solid State Ionics* **152-153**, 783-800.

Rodríguez-González L., Simon U. (2010) NH_3-TPD measurements using a zeolite-based sensor, *Measurement Science and Technology* **21**, 027003.

Rose D., Boger T. (2009) Different Approaches to Soot Estimation as Key Requirement for DPF Applications, *SAE Paper* 2009-01-1262.

Sappok A., Bromberg L., Parks J., Prikhodko V. (2010) Loading and Regeneration Analysis of a Diesel Particulate Filter with a Radio Frequency-Based Sensor, *SAE Paper* 2010-01-2126.

Schuler A., Votsmeier M., Kiwic P., Gieshoff J., Hauptmann W., Drochner A., Vogel H. (2009) NH_3-SCR on Fe zeolite catalysts – From model setup to NH_3 dosing, *Chemical Engineering Journal* **154**, 333-340.

Shelef M., McCabe R.W. (2000) Twenty-five years after introduction of automotive catalysts: What next? *Catalysis Today* **62**, 35-50.

Simon U., Flesch U., Maunz W., Müller R., Plog C. (1998) The effect of NH_3 on the ionic conductivity of dehydrated zeolites Na beta and H beta, *Microporous and Mesoporous Materials* **21**, 111-116.

Sucher M., Fox J. (1963) Handbook of Microwave Measurements, *Polytech. Inst. Brooklyn*, 3rd ed., Brooklyn.

Takeuchi M., Matsumoto S. (2004) NO_x storage-reduction catalysts for gasoline engines, *Topics in Catalysis* **28**, 151-156.

Twigg M.V. (2007) Progress and future challenges in controlling automotive exhaust gas emissions, *Applied Catalysis B: Environmental* **70**, 2-15.

Twigg M.V., Phillips P.R. (2009) Cleaning the air we breathe—Controlling Diesel particulate emissions from passenger cars, *Platinum Metals Review* **53**, 27-34.

Walton F.B. (2007) Method and system for detecting soot and ash concentrations in a filter, *US Patent Specification* US 7,157,919.

Zhuiykov S., Miura N. (2007) Development of zirconia-based potentiometric NOx sensors for automotive and energy industries in the early 21st century: What are the prospects for sensors? *Sensors and Actuators B: Chemical* **121**, 639-651.

Manuscript accepted in October 2013
Published online in April 2014

Cite this article as: R. Moos and G. Fischerauer (2015). Automotive Catalyst State Diagnosis Using Microwaves, *Oil Gas Sci. Technol* **70**, 1, 55-65.